

## Chapter 2

# Ground State Calculations for Protonated PAHs

### 2.1 Introduction

*Ab initio* ground electronic state calculations can be used to determine geometries and energies of all possible protonated PAH isomers and thereby examine whether there are common properties and general trends among this class of compounds. In addition, the stability and allowed dissociation channels need to be investigated to guide the interpretation of the spectroscopic data presented later in this thesis, while the geometries serve as the starting point for calculation of the energies of excited electronic states.

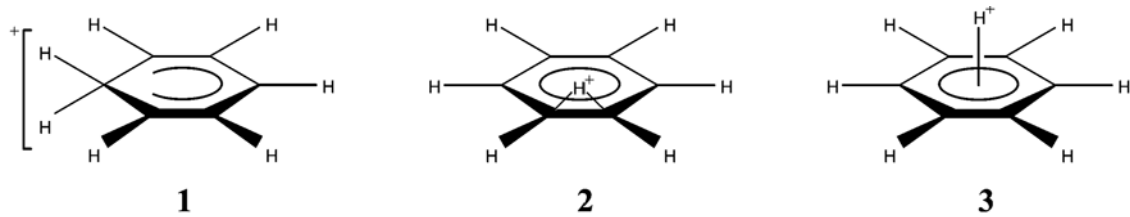


Figure 2.1: Structures for protonated benzene PES stationary points. Adapted from [3].

There have been a number of quantum chemical calculations performed on the structures of protonated benzene [92–95]. Three stationary points on its potential energy surface were

identified (Figure 2.1). They are the  $\sigma$  complex structure (1), the  $\text{H}^+$  bridged structure (2), and a  $\pi$  complex of benzene and  $\text{H}^+$  (3). Structure (1) is the global minimum (the most stable form) and the other two are first and second order transition states, respectively. Their relative energies were calculated to be 0, 6.4 and 49.3 kcal/mol [3].

Fairly low level results on the structures of stable isomers for selected protonated PAHs (naphthalene, pyrene, coronene, circumcoronene) and their vibrational spectra have also been calculated [23]. An extensive suite of quantum chemical calculations for benzene, naphthalene, anthracene, phenanthrene and pyrene is presented in this chapter. Although benzene is technically not a PAH molecule, it was considered here as a well-studied aromatic test system. Before turning to the results themselves, the nomenclature of protonated PAHs and the computational approach will be covered first.

## 2.2 Methodology

### 2.2.1 Naming Conventions

The naming of different isomers of protonated PAHs is based on the IUPAC nomenclature of neutral PAHs. Figure 2.2 outlines the conventional numbering of carbon atoms in neutral PAHs. The numbers in **bold** depict the stable isomers of protonated PAHs. Fusion carbon atoms at the juncture of two aromatic rings are usually not numbered, but they are referenced in certain calculations, especially for protonated naphthalene and anthracene. These atoms are therefore labeled with numbers in *italics*.

For protonated PAHs, the naming system is illustrated by the following example: when  $\text{H}^+$  is attached to C atom number 1 of naphthalene or C atom number 9 of anthracene, for example, the 1–hydronaphthalene and 9–hydroanthracene cations are formed, respectively.

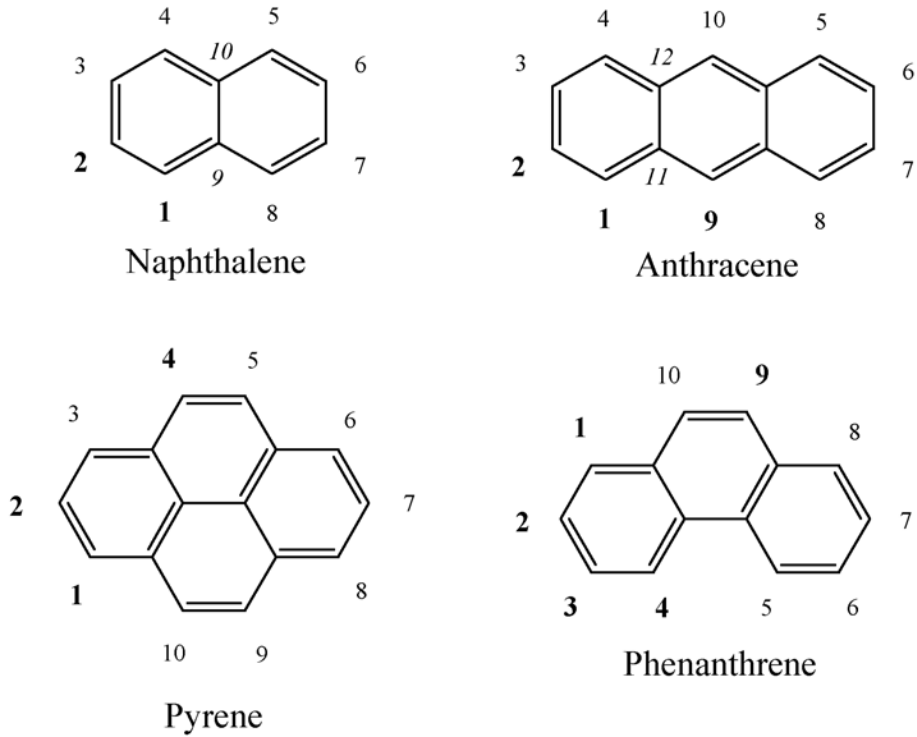


Figure 2.2: Carbon atom numbering conventions for neutral PAHs.

For simplicity, in this thesis the notation isomer 1 of protonated naphthalene and isomer 9 of protonated anthracene, or  $1\text{-C}_{10}\text{H}_9^+$  and  $9\text{-C}_{14}\text{H}_{11}^+$  will be used. The notation  $1\rightarrow 2\text{ C}_{10}\text{H}_9^+$  thus designates a transition state between  $1\text{-C}_{10}\text{H}_9^+$  and  $2\text{-C}_{10}\text{H}_9^+$ , while  $6\rightarrow 1\text{ C}_{10}\text{H}_8^+$  describes  $1\text{-C}_{10}\text{H}_9^+$  with a hydrogen atom removed from carbon number 6 of naphthalene. This is an isomer of naphthalene cation, where a hydrogen atom has been moved from carbon atom 6 to carbon atom 1. Similarly,  $1\text{-C}_{10}\text{H}_7^+$  designates the naphthalene cation with a hydrogen atom removed from the carbon 1 position.

### 2.2.2 Software

Contemporary desktop personal computer (PC) systems are now sufficiently powerful to perform *ab initio* calculations on moderately complex systems in reasonable times. Although

they are not as powerful as mainframe systems, they are very attractive from the price and availability perspective. GAUSSIAN 98, Revision A.9 [98] (the most widely used version) for Microsoft Windows was used to carry out all calculations mentioned below.

### 2.2.3 Choice of the Computer System

Most central processing units (CPUs) on the PC market are manufactured by Intel and Advanced Microdevices (AMD). Software performance depends strongly on the computer hardware, the most important of which is the CPU (specifically its architecture and clock speed). A few tests were therefore performed to determine the best performing PC for GAUSSIAN calculations and consisted of two different calculations (italics below correspond to commands within GAUSSIAN 98):

The first test was to optimize the geometry of isomer 1 of protonated anthracene:

```
# Opt=(CalcAll,Tight,GDIIS) rB3LYP/6-311++G(d,p) Guess=Mix
```

This calculation is performed mostly in memory and takes about 24 hours.

The second calculation was to optimize the geometry of protonated benzene:

```
# Opt rMP2/6-311+G(d,p) Guess=Mix
```

This calculation takes only about 1.5 hours, but carries out substantial read/write operations with the hard drive.

The following PC systems, differing mostly by CPU type, were tested:

**P4–3.6** – CPU Intel Pentium 4, 3.4 GHz running at 3.67 GHz (8% overclock), RAM 1 Gb Dual DDR 433 (2×433 MHz), Hard drive ATA–5 (133Mb/s), Windows XP SP1.

**P4–2.7** – CPU Intel Pentium 4, 2.66 GHz running at 2.72 GHz (2.26% overclock), RAM 1 Gb RDRAM (1066 MHz), Hard drive ATA–5 (133 Mb/s), Windows XP SP1.

**A–XP** – CPU AMD Athlon XP, 2800+ running at 2.11 GHz (0% overclock), RAM 1 Gb

Dual DDR 333 ( $2 \times 333$  MHz), Hard drive SATA (150 Mb/s), Windows 2000 SP4.

**A-64** – CPU AMD Athlon 64, 3000+ running at 2.10 GHz (5% overclock), RAM 1 Gb DDR 433 (433 MHz), Hard drive ATA-5 (133 Mb/s), Windows XP SP1.

Results for each system are presented in Table 2.1 from which it is clear that at present, PCs with Intel Pentium 4 CPUs run GAUSSIAN 98 calculations faster than AMD Athlon CPUs, rated for approximately the same equivalent clock speed. Almost all calculations described in this thesis were performed on the P4-2.7 and P4-3.6 systems.

Table 2.1: PC performance tests with GAUSSIAN 98.

PC System	P4-3.6	P4-2.7	A-XP	A-64
CPU Clock, MHz	3638	2720	2112	2100
Equivalent CPU Clock Rating, MHz	3638	2720	2800	3150
In-memory job, s	63900	86286	106568	–
High disk swap job, s	4536	5484	7102	5665

## 2.2.4 Theory Level and Basis Set

Density functional theory (DFT) [99,100] has proven to be a good alternative to Linear Combination of Atomic Orbitals-Molecular Orbital (LCAO-MO) *ab initio* methods, especially for aromatic hydrocarbons. The advantages of DFT calculations are in their speed and smaller computer resource requirements. One such method denoted B3LYP (Becke three-parameter functional [101] with Lee-Yang-Parr correlation functional [102]) was used in previous calculations of protonated PAH structures [23] and has been selected here to optimize the geometries and calculate vibrational frequencies of several systems.

The basis set was constrained to be the same for all molecules studied, with a calculation limit of no more than 1 week chosen to define the basis set size. For the largest molecule studied – protonated pyrene – the biggest basis set is 6-311++G\*\* (McLean-Chandler 6-311G basis set [103,104] with polarization functions (d,p) [105] and diffuse functions

++ [106]).

In addition to being faster, DFT performs most integral calculations in memory and requires little swap space on the computer hard drive. For comparison, the Møller-Plesset MP2 6–311++G(d,p) method on protonated benzene uses about 10 Gb of the swap space. For protonated naphthalene at the same theory level and basis set, the required amount of the swap space would exceed 16 Gb which is the maximum allowed by 32-bit versions of GAUSSIAN 98.

Geometry optimization was performed in a few steps, where the basis set size was slowly increased to speed convergence. At the largest basis set, the vibrational frequencies were calculated as a part of the optimization process. The total calculational procedure was as follows:

1. A model of the molecule was built in the GAUSSIAN 98 visualization package GaussView, version 2.1 [107].
2. The geometry was optimized with the 6–31G basis set.
3. The geometry was optimized with the 6–31+G(d) basis set.
4. The geometry was optimized with the 6–311G(d,p) basis set.
5. The geometry was optimized with the 6–311++G(d,p) basis set.

In step 5, the specific calculation call was:

```
# Opt=(CalcAll,Tight,GDIIS) B3LYP/6-311++G(d,p) NoSymm Guess=Mix
```

Options *CalcAll*, *Tight* and *GDIIS* were used to assure better convergence, while *CalcAll* was used to predict the frequencies and intensities of IR-active vibrational modes. The *NoSymm* switch proved important in stabilizing the convergence criteria for molecules with rotational symmetry, especially neutral PAHs and their cations.

## 2.3 Geometries

### 2.3.1 Protonated Benzene, Naphthalene, Anthracene and Pyrene

Appendix A (Tables A.2 – A.20) contains GAUSSIAN Z-matrices for the optimized geometries of neutral benzene, naphthalene, anthracene and pyrene, as well as stable isomers of their protonated forms. The calculated dipole moments, A, B and C rotational constants, and derived molecular symmetry groups are also listed there (Table A.1).

Protonated benzene  $C_6H_7^+$  has only one isomer, while the transition state for isomerization (1–2  $C_6H_7^+$ ) is that of the bridged structure (2) from Figure 2.1. Molecular models of these structures are shown in Figure 2.3.

Protonated naphthalene has two principal isomers: 1– and 2– $C_{10}H_9^+$  (Figure 2.4). An additional isomer 9– $C_{10}H_9^+$  is much higher in energy and has a very low barrier for isomerization into 1– $C_{10}H_9^+$ . Thanks to the increasing number of isomers, there are now several isomerization transition states: 1–2, 2–3 (not shown), 1–9 and 9–10.

Protonated anthracene has three main principal isomers: 1–, 2– and 9– $C_{14}H_{11}^+$ . Again, the 11– $C_{14}H_{11}^+$  isomer is much higher in energy and has a very low barrier for isomerization into 9– $C_{14}H_{11}^+$ . Figure 2.5 presents a number of molecular models of these isomers and the 1–2, 2–3 (not shown), 1–11 (not shown), 9–11 and 11–12(not shown) transition states accessed by proton tunneling or hopping.

Protonated phenanthrene has five stable isomers: 1–, 2–, 3–, 4– and 9– $C_{14}H_{11}^+$  (Figure 2.6). Thanks to the much more complex potential energy surface, higher energy isomers and transition states are not considered here.

Protonated pyrene has three main isomers: 1–, 2– and 4– $C_{16}H_{11}^+$  (Figure 2.7). Less stable isomers and transition states are not considered here.

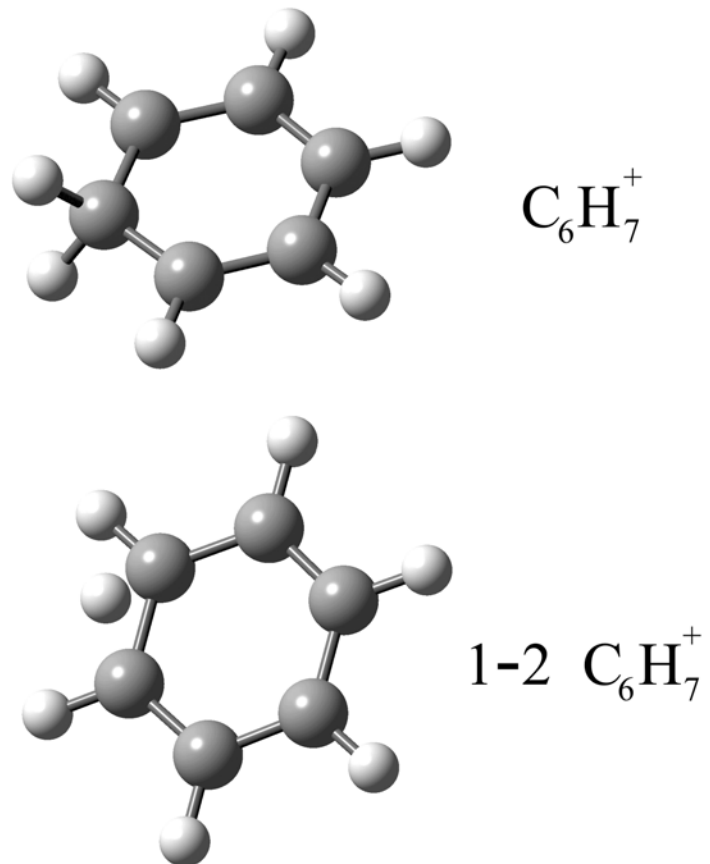


Figure 2.3: Structures of protonated benzene  $\text{C}_6\text{H}_7^+$  and its isomerization transition state  $1-2 \text{ C}_6\text{H}_7^+$ .

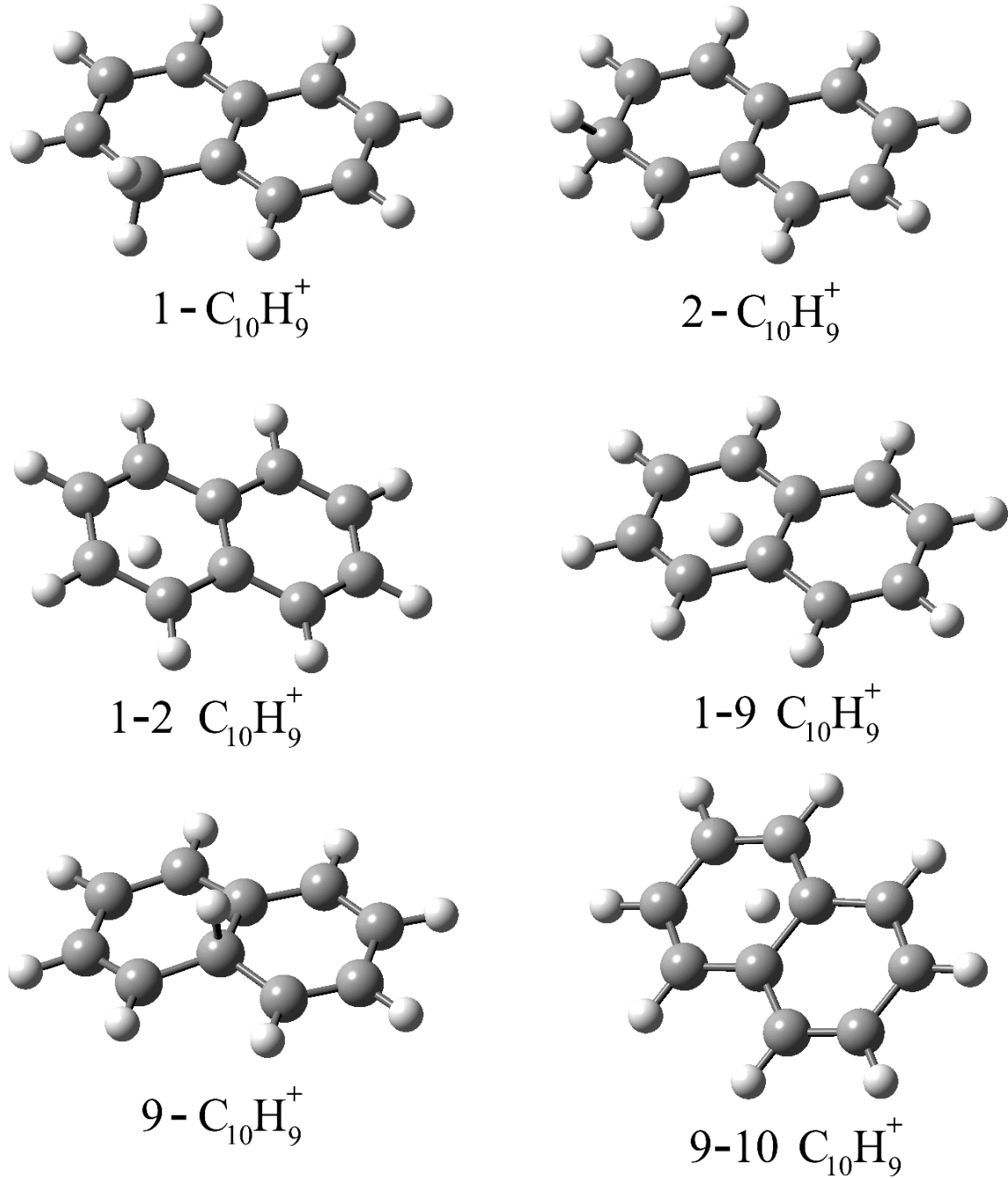


Figure 2.4: Structures of the protonated naphthalene C<sub>10</sub>H<sub>9</sub><sup>+</sup> isomers 1,2 and 9, along with three of the isomerization transition states that connect them.

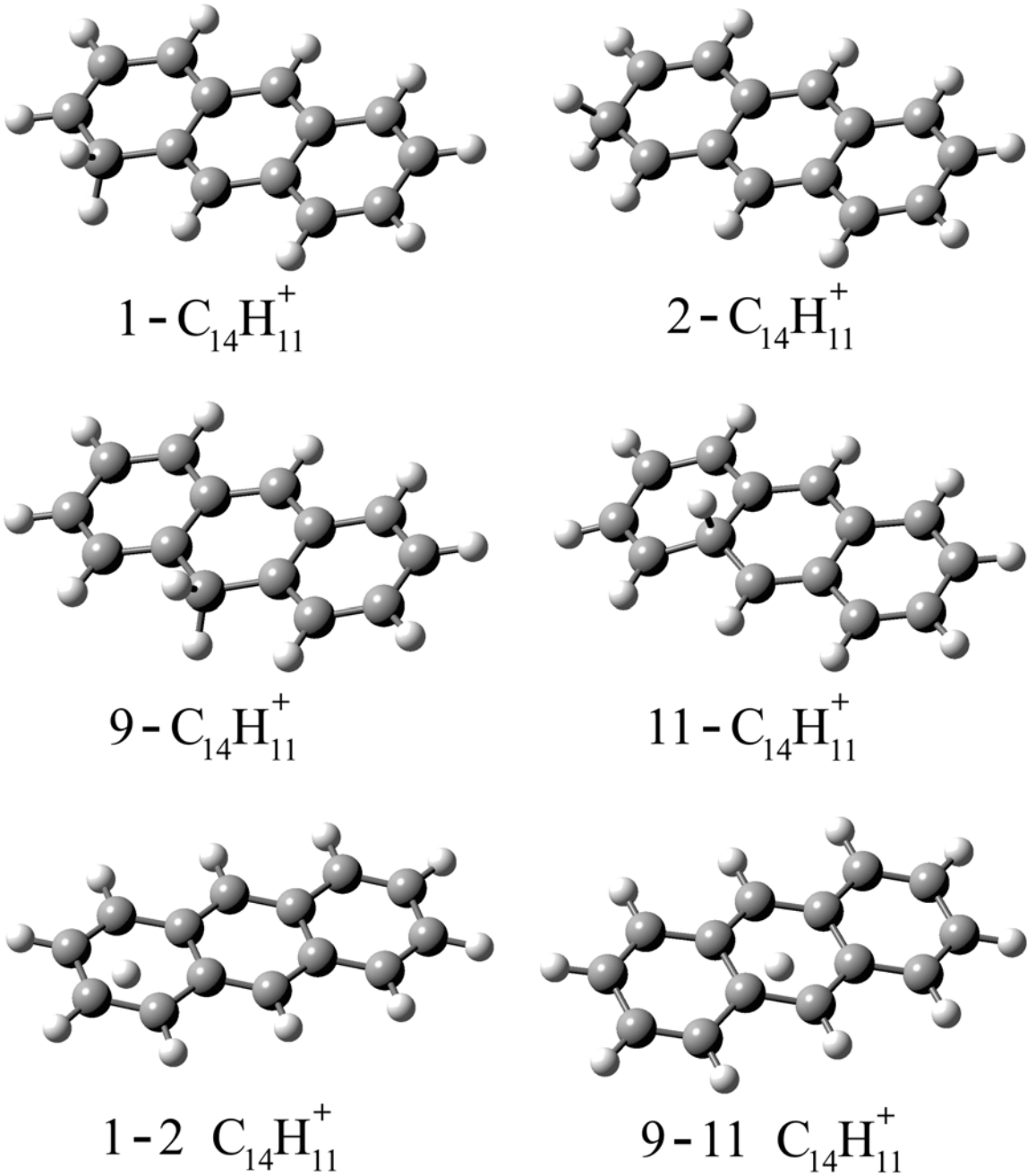


Figure 2.5: Structures of the protonated anthracene  $\text{C}_{14}\text{H}_{11}^+$  isomers 1, 2, 9 and 11, along with two of the lowest barrier isomerization transition states.

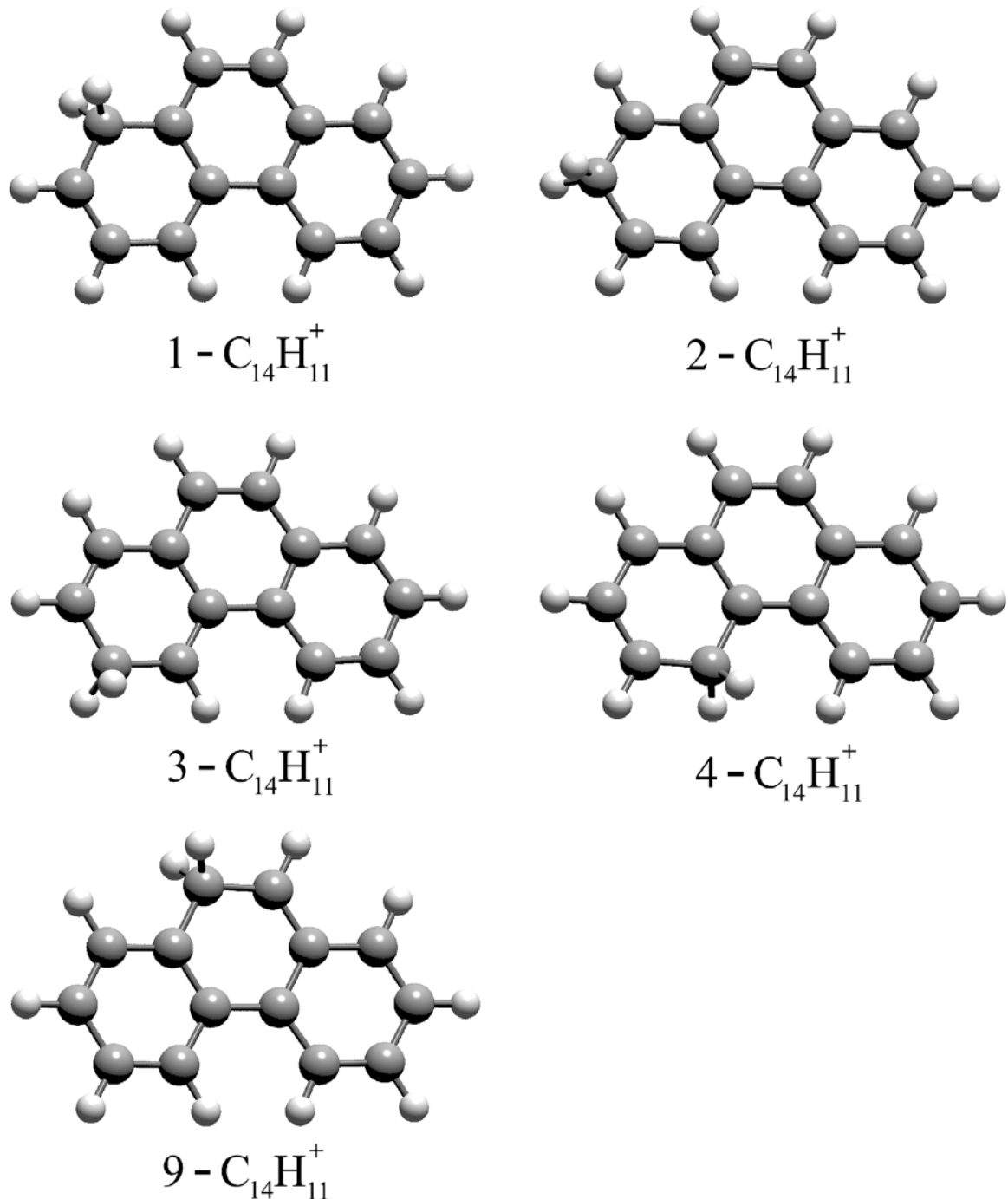


Figure 2.6: Structures of the protonated phenanthrene  $\text{C}_{14}\text{H}_{11}^+$  isomers 1, 2, 3, 4 and 9.

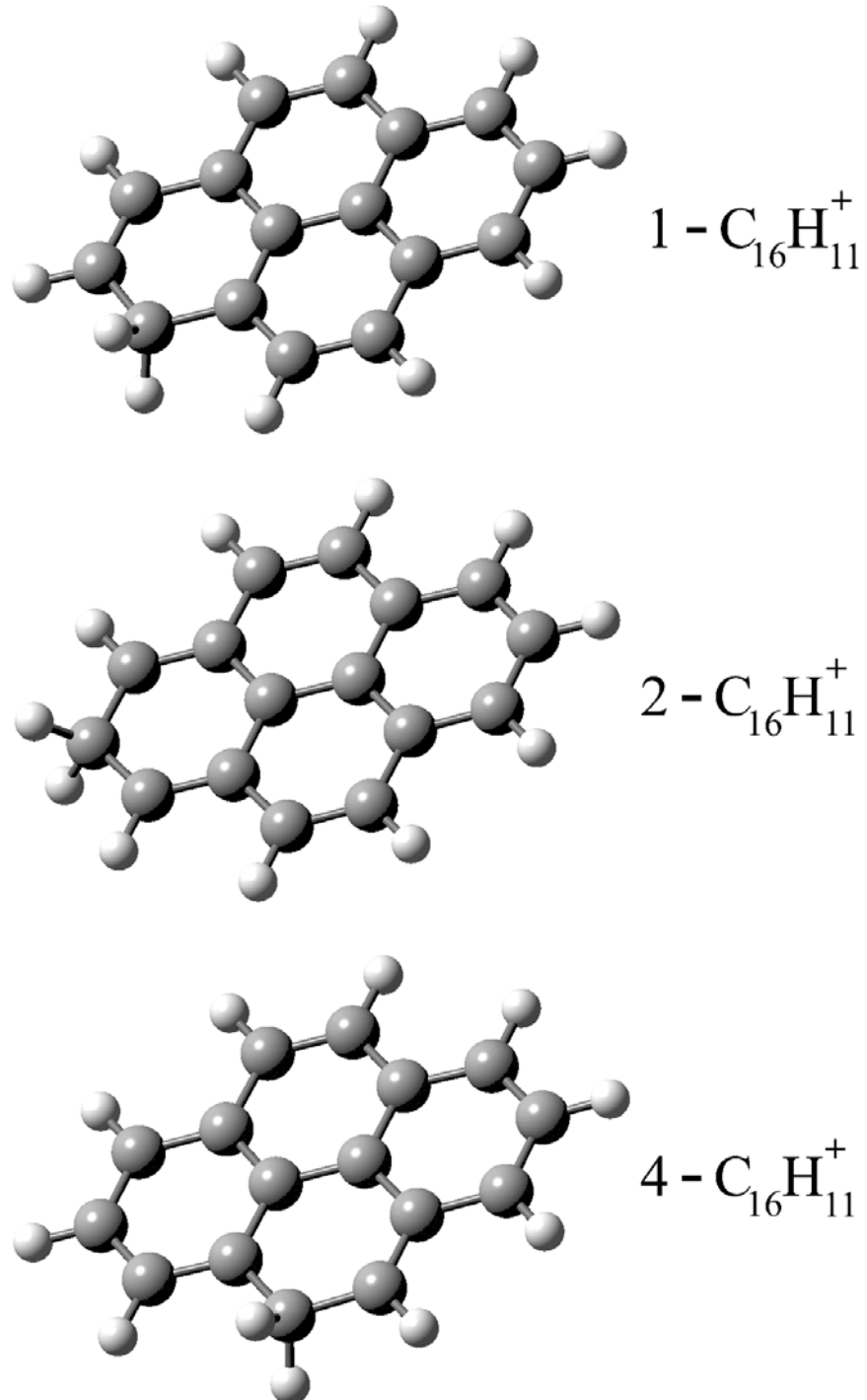


Figure 2.7: Structures of the protonated pyrene  $\text{C}_{16}\text{H}_{11}^+$  isomers 1, 2 and 4.

### 2.3.2 Typical Geometry Changes Upon Protonation

Small but noticeable geometrical changes occur upon the protonation of aromatic hydrocarbons. In stable isomers, the proton binds to the carbon atom, forming a  $\sigma$  complex and changing the hybridization from  $sp^2$  to  $sp^3$ . C–C bonds for the  $sp^3$  carbon elongate due to electron density redistribution by  $0.07 - 0.12 \text{ \AA}$ , while C–C bonds for an adjacent  $sp^2$  carbon atom shorten by  $0.02 - 0.06 \text{ \AA}$  (Figure 2.8 – 1). For  $\text{CH}_2$  sites, the lengths of the C–H bonds are predicted to be  $1.10 \text{ \AA}$ —somewhat longer than the  $1.085 \text{ \AA}$  predicted for the CH sites. The H–C–H angle values for  $\text{CH}_2$  sites are in the range  $100 - 104$  degrees.

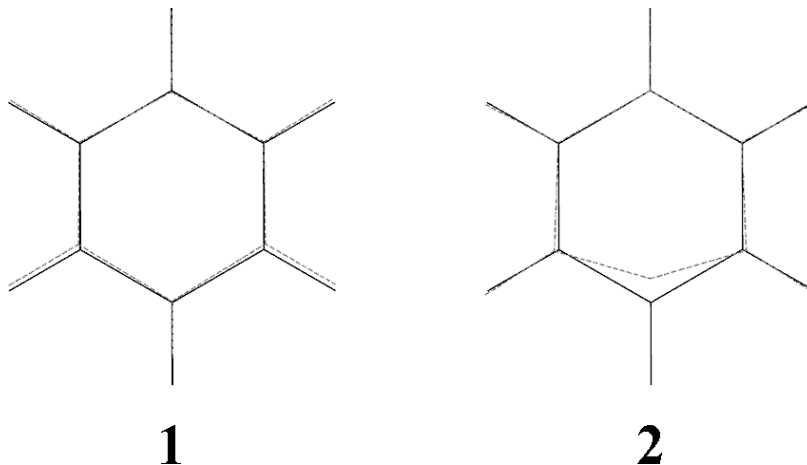


Figure 2.8: Benzene geometry changes (dashed line). 1 – during protonation, 2 – during cation dehydrogenation.

The carbon backbone of the protonated molecule is predicted to remain planar. A few ‘flatness’ tests were performed with protonated naphthalene and anthracene, where the initial geometries of ions were set to resemble cyclohexane. Geometry optimization was then performed with the MP2 and B3LYP methods using different size basis sets. The convergence to a true minimum, not a saddle point on the potential energy surface, was verified by making sure that all vibrational eigenfrequencies were real. In each of these

tests, all carbon atoms settled into a plane. Thus, the protonated PAHs are predicted to have either  $C_s$  or  $C_{2v}$  symmetry, depending on the isomer (Appendix A, Table A.1).

The less stable isomers, where the proton binds to a ring fusion carbon, are no longer planar thanks to changes in the hybridization at the protonation site. In the transition states, the carbon backbone bends out-of-plane by a small amount. For transition states that do not involve fusion carbons, the change in the dihedral angle is only 1 degree. For transition states with fusion carbon, the bending distortion is closer to 5 degrees.

### 2.3.3 Geometries of Dehydrogenated PAH Cations

As described below, the properties of various forms of dehydrogenated PAHs may be important in catalytic cycles that can form molecular hydrogen in the diffuse interstellar medium. Here, only the geometries of benzene, naphthalene and anthracene dehydrogenated cations were calculated as a first step in the consideration of such cycles. Theoretically, the dehydrogenated carbon atom is being pulled closer to the middle of the ring. This leads to an increase of the C–C–C angle at the dehydrogenation site from  $120^\circ$  to  $143 - 149^\circ$ , and a decrease in the adjacent C–C–C angles to  $102 - 108^\circ$  (Figure 2.8 – 2).  $C_6H_5^+$  and  $1-C_{10}H_7^+$  remained flat, while the other dehydrogenated cations considered were found to distort from the planar symmetries of the protonated PAHs.

### 2.3.4 Geometries of Hydrogenated and Dehydrogenated PAHs

Due to their low ionization energies, atomic carbon and many carbonaceous species are expected to be ionized in diffuse interstellar clouds. The amount of free electrons in these objects is then approximately the same as the amount of carbon, and electron recombination may be one of the major ways of removal for protonated PAHs. Geometries for singly

hydrogenated and dehydrogenated benzene, naphthalene, and anthracene are calculated as a part of the recombination process investigation.

From all of the considered hydrogenated PAHs which essentially are neutralized protonated PAHs, the carbon backbone was not planar only in 9-C<sub>14</sub>H<sub>11</sub>. C–C bonds of the hydrogenation site were longer by  $\sim$ 0.01 Å and the H–C–H angle was  $\sim$ 1° larger than in protonated PAHs. The rest of the geometry was similar to protonated PAHs.

All considered dehydrogenated PAHs had planar geometries. Dehydrogenation would typically result in the radical site carbon atom retraction into the ring, which led to C–C bond shortening by  $\sim$ 0.02 – 0.03 Å.

## 2.4 Calculated Values

### 2.4.1 Vibrational Frequencies

As was mentioned above, the vibrational frequencies and IR intensities of the protonated PAH isomers were calculated here as a part of the geometry optimization. The effect of the level of theory and basis set size on the calculated vibrational frequencies of organic molecules has been studied previously [108–110]. Typically, the calculated vibrational frequencies are larger than the experimental values due to the harmonic nature of the *ab initio* estimate. Thus, the predicted vibrational frequencies must be scaled down by modest amounts to agree with the experiment. The actual scaling factor depends on the level of theory employed, the basis set, and the type of vibration.

To derive the scaling factors for the B3LYP 6–311++G(d,p) calculations presented here, the vibrational frequencies were calculated for neutral benzene and anthracene and compared to the experimental gas phase frequencies [111, 112]. A detailed comparison of

the results are presented in Appendix A (Tables A.21, A.22), which shows that the scaling factors are  $\sim 0.962$  for C–H stretching vibrations (frequencies above  $2000\text{ cm}^{-1}$ ) and  $\sim 0.982$  for the rest. These scaling factors were then used to determine vibrational frequencies of protonated PAHs, neutral PAHs and their cations and to thereby calculate the zero point vibrational energy (ZPE) content of all molecules and ions. The ZPE values were then used to correct the relative energies of isomers and reaction channels (2.5). The full list of the scaled vibrational frequencies for neutral and protonated PAHs is listed in Appendix A (Tables A.23 – A.27) along with the IR vibrational spectra in stick form (Figures A.1 – A.19). In the latter figures, the height of the vertical lines in each spectrum depicts the IR intensities. As a comparison, similar spectra for protonated naphthalene and pyrene convoluted with  $20\text{ cm}^{-1}$  linewidth to simulate interstellar spectra were reported in [23].

#### 2.4.2 Proton Affinities

As a part of the ground state energy calculations, the proton affinities for the neutral PAHs were estimated. The resulting values were a good measure of the precision of the calculations. Here, the proton affinities were calculated as an energy difference between the neutral PAH (equivalently, a geometry for  $\text{PAH}-\text{H}^+$  where the proton is far from the molecule) and the isomers of the protonated PAHs (where the proton is bound to the molecule). These values were then compared with the available experimental values [113, 114]. It should be noted that for molecules with more than one protonation site, it is theoretically possible to calculate the properties for individual isomers, while the experimental data necessarily average over the isomers present in the laboratory. For anthracene and pyrene, the predicted variation in proton affinity is large, with the experimental value nicely bracketed by theory. As one can see from Table 2.2, the match is  $\sim 2 - 3\text{ kcal/mol}$ , or approximately a

1.5% difference. Hence, the relative values of the energy levels may be trusted to roughly this level.

Table 2.2: Experimental and calculated proton affinities of neutral aromatics.

Molecule	Experimental (kcal/mol)	Calculated (kcal/mol)	$H^+$ site
Benzene	179.3	182.19	1
Naphthalene	191.9	196.20	1
		193.30	2
Anthracene	209.7	203.84	1
		200.80	2
		212.50	9
Phenanthrene	197.3	199.80	1
		197.80	2
		199.25	3
		198.73	4
		199.60	9
Pyrene	207.7	211.24	1
		197.02	2
		200.98	4

### 2.4.3 Ionization Energies

Ionization energies are calculated as the energy difference between the cation and neutral molecule, and were corrected by the ZPE values. The results are compared with the experimental ionization energies [113] for benzene [65, 66], naphthalene [68, 70], anthracene [69], phenanthrene and pyrene [115] in Table 2.3. The calculated values are consistently lower than experiment by  $\sim 0.3$  eV (6.9 kcal/mol), but the differences predicted here are not as

Table 2.3: Experimental and calculated ionization energies of neutral aromatics.

Molecule	Experimental (eV)	Calculated (eV)
Benzene	9.24378	9.0562
Naphthalene	8.1442	7.8655
Anthracene	7.4233	7.1002
Phenanthrene	7.891	7.5845
Pyrene	7.426	7.1427

large as for those calculated previously with the B3LYP 4–31G method [116].

Ionization energies were also calculated for hydrogenated and dehydrogenated benzene, naphthalene, and anthracene (Appendix A, Table A.36). The typical values for hydrogenated PAHs were in the range of 6.2 – 6.4 eV, which is lower than for neutral PAHs. For deprotonated PAHs, the values were higher (in the 7.7 – 8.0 eV range). If any of these species are present in diffuse interstellar clouds, they should be promptly ionized, yielding protonated PAHs and dehydrogenated PAH cations respectively.

For isomer 2 of protonated naphthalene, the ionization energy needed to yield a doubly charged ion was calculated in order get an idea of the likely range of values for protonated PAHs. The calculated value is 12.9147 eV, 297.81 kcal/mol. Photons below the ionization threshold of 13.6 eV for hydrogen atoms are widely present in the diffuse interstellar medium. This calculation suggests that doubly charged PAH species will need to be considered in models of the charge states of PAHs in the galaxy.

## 2.5 Energy Landscapes

The energy landscape diagrams for protonated PAHs were investigated thoroughly in order to compare the energetics of different isomers and possible dissociation channels. These calculations serve two main goals. First, it is essential to find the difference in the stability of different isomers in their ground state for the same protonated PAH molecule, including the heights of the isomerization barriers. This information, together with the excited states calculations presented in Chapter 3, are essential to the interpretation of the experimental data on the photophysical and electronic state properties of protonated PAHs (Chapters 5 and 6). Second, since photodissociation was chosen as a method for recording the spectra of protonated PAHs, it is important to know which dissociation channels are

feasible, their energetics, and their Franck-Condon overlap with the ground state(s).

In all energy landscape diagrams below, the energy of the lowest dissociation channel was set as the energy zero. Hence, in this energy scale, the stable isomers have negative energies.

### 2.5.1 Protonated Benzene

Isomerization and dissociation calculations on protonated benzene have been performed numerous times [92–95]. At the level of theory employed here, the only isomer of protonated

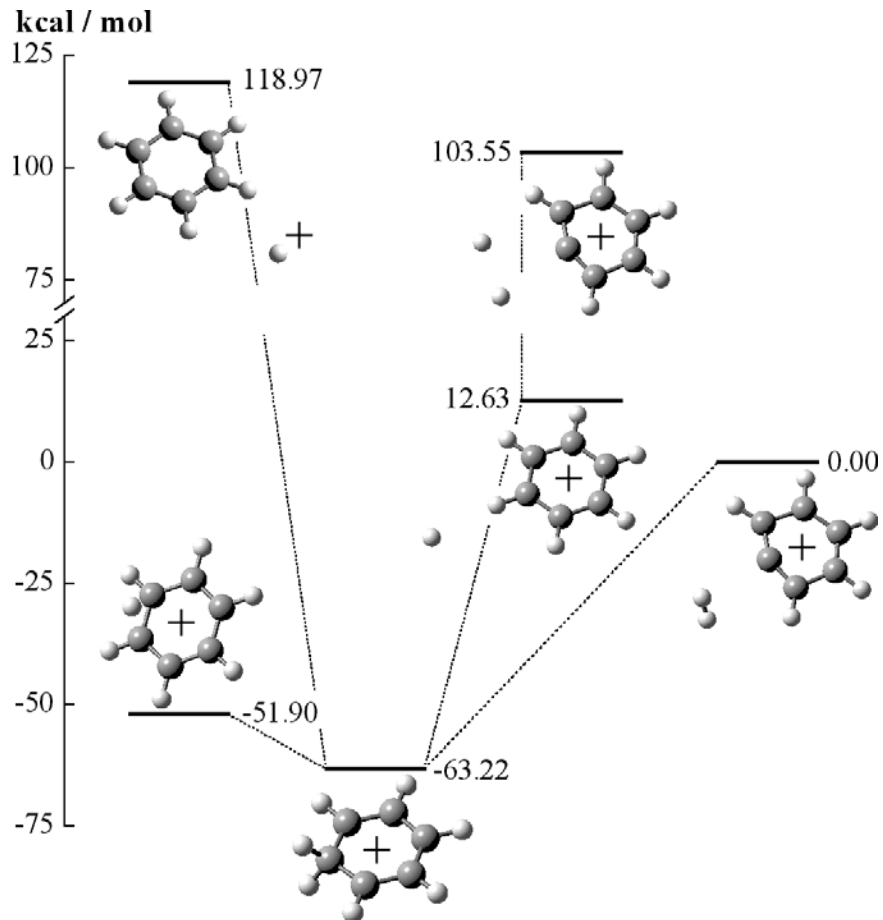


Figure 2.9: The energy landscape for protonated benzene.

benzene is stable with respect to dissociation by 63.22 kcal/mol (Figure 2.9, Table A.28 in Appendix A). The only possible 1–2 isomerization results in the identical isomer and has a barrier height of 11.32 kcal/mol.

The lowest dissociation channels are predicted to occur through the loss of an H<sub>2</sub> molecule (0.00 kcal/mol) or a hydrogen atom (12.63 kcal/mol) from the protonation site. The loss of H<sub>2</sub> most likely has a barrier, but the barrier height was not calculated here due to the difficulty of locating the transition state geometry. The H atom loss channel does not appear to have a barrier. A sequential loss of two hydrogen atoms is much higher in energy than the loss of H<sub>2</sub> molecule. Finally, the loss of an H atom from CH sites and the cleavage of C–C bonds are not considered here as they lie much higher in energy. In addition, the loss of the proton from the CH<sub>2</sub> site lies 118.97 kcal/mol above the lowest dissociation channel – a very large number! Thus, the protonation of neutral benzene in the gas phase cannot occur by simply attaching a proton to it. Thus, the more favorable protonation mechanism in the interstellar medium occurs via proton transfer from H<sub>3</sub><sup>+</sup> in dense clouds or through the radiative association reaction of PAH radical cations with atomic hydrogen in the diffuse clouds. A sequential loss of two H atoms, with the first H atom arising from the CH<sub>2</sub> site, followed by C–H bond cleavage, is 103.55 kcal/mol above the lowest dissociation channel. Such a dissociation pathway would only be possible for very highly vibrationally excited species.

### 2.5.2 Protonated Naphthalene

The energetics of the reaction between the naphthalene cation (C<sub>10</sub>H<sub>8</sub><sup>+</sup>) and an H atom, and the energies for isomers 1 and 2 of protonated naphthalene and the isomerization barrier between them, have been calculated previously at the B3LYP 4–31G level [23, 117]. The

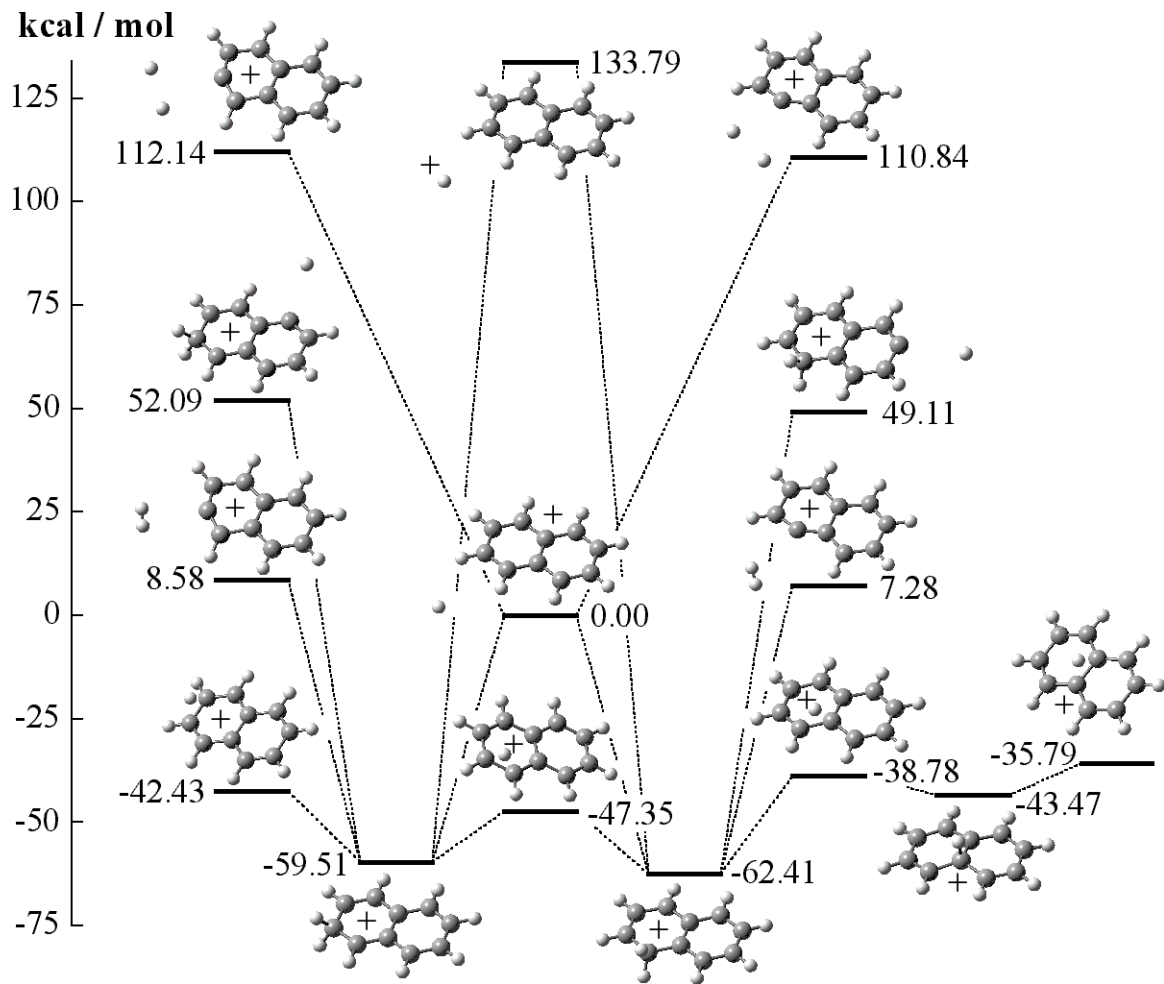


Figure 2.10: The energy landscape of protonated naphthalene.

two isomers of protonated naphthalene are stable with respect to dissociation by 62.41 kcal/mol ( $1\text{-C}_{10}\text{H}_9^+$ ) and 59.51 kcal/mol ( $2\text{-C}_{10}\text{H}_9^+$ ), respectively (Figure 2.10, Table A.29 in Appendix A). Isomer 2 can undergo 2–3 isomerization into an identical isomer (through a barrier of 17.08 kcal/mol) and 2–1 isomerization into the more stable  $1\text{-C}_{10}\text{H}_9^+$  isomer (barrier height 12.06 kcal/mol). Given sufficient energy, proton hopping can convert isomer 1 into isomer 2 (barrier height 15.06 kcal/mol) and isomer 9 (barrier height 23.63 kcal/mol) in which the proton is bound to a ring fusion carbon. Energetically, isomer 9 is less stable than isomer 1 by 18.94 kcal/mol and has a low barrier for 9–1 or 9–8 isomerization (barrier

height 4.69 kcal/mol). It can also undergo 9–10 isomerization across the ring fusion into an identical isomer (barrier height 7.68 kcal/mol). Thus, it is unlikely that isomer 9 would be important under interstellar conditions.

The lowest dissociation channel for protonated naphthalene is the loss of an H atom from the protonation site (0.00 kcal/mol). The next – not so distant in energy – occurs via the loss of H<sub>2</sub> from the protonation site (7.28 kcal/mol for isomer 1 and 8.58 kcal/mol for isomer 2). The energies for the loss of H atom from C–H sites (not the protonation sites) were calculated as well. As for protonated benzene, they are substantially higher in energy: 49.11 ± 1.36 kcal/mol for isomer 1 (for a full listing see Table A.29 in Appendix A) and 52.09 ± 1.39 kcal/mol for isomer 2 (c.f. the bottom part of Table A.29 in Appendix A). The CH site dissociation channels of protonated naphthalene are therefore unlikely to be important in the interstellar medium. The loss of a proton from the CH<sub>2</sub> site is 133.79 kcal/mol above the lowest dissociation channel. Finally, the sequential loss of two H atoms, first from the CH<sub>2</sub> site and then another H atom, has energies of 110.84 kcal/mol (for isomer 1) and 112.14 kcal/mol (for isomer 2) above the lowest dissociation channel.

### 2.5.3 Protonated Anthracene

Protonated anthracene has three isomers that are stable with respect to dissociation by 52.41 kcal/mol (1-C<sub>14</sub>H<sub>11</sub><sup>+</sup>), 49.36 kcal/mol (2-C<sub>14</sub>H<sub>11</sub><sup>+</sup>) and 61.06 kcal/mol (9-C<sub>14</sub>H<sub>11</sub><sup>+</sup>) (Figure 2.11, Table A.30 in Appendix A), respectively. Isomer 2 can undergo 2–3 isomerization into an identical isomer (barrier height 21.20 kcal/mol) and 2–1 isomerization (barrier height 14.49 kcal/mol). The reverse 2–1 isomerization has a barrier height of 17.54 kcal/mol, while the 1–11 isomerization must surmount a barrier height of 27.84 kcal/mol in order to place the proton at a ring fusion carbon. Energetically, isomer 11 is less stable

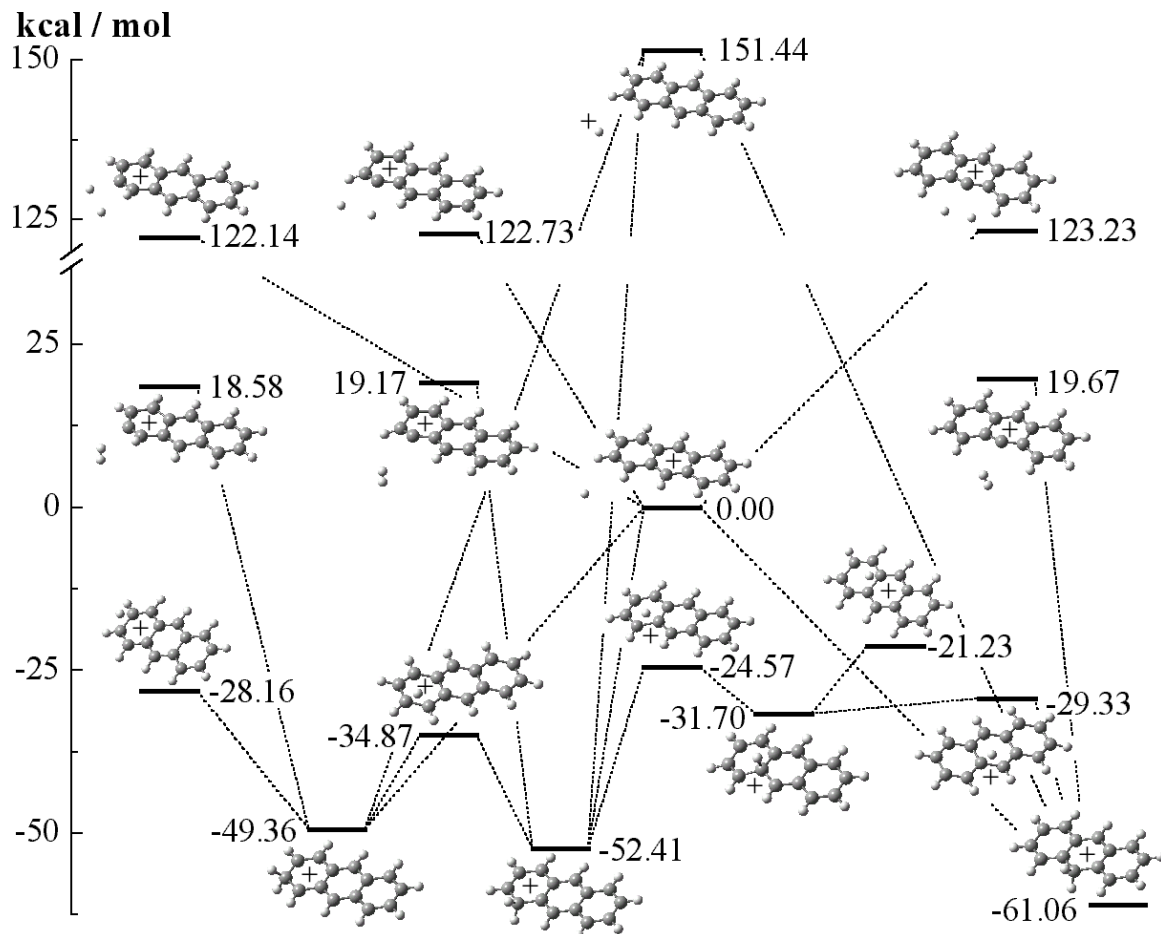


Figure 2.11: Protonated anthracene energy landscape.

than isomer 1 by 20.70 kcal/mol and has a very low barrier for 11–9 isomerization into the most stable isomer 9 (barrier height 2.37 kcal/mol). As with protonated naphthalene, it is therefore unlikely that the ring fusion isomer would be an important DIB carrier. Isomer 11 can also undergo 11–12 isomerization across the ring fusion into an identical isomer (barrier height 10.47 kcal/mol). Isomer 9 can undergo only 9–11 isomerization (barrier height 31.73 kcal/mol).

The lowest dissociation channel for protonated anthracene is the loss of an H atom from the protonation site (0.00 kcal/mol). The loss of an H<sub>2</sub> molecule from the protonation site is nearly isoenergetic for all three isomers (19.17 kcal/mol for isomer 1, 18.58 kcal/mol

for isomer 2 and 19.67 kcal/mol for isomer 9). The loss of a proton from the CH<sub>2</sub> site is again quite unfavorable at an energy of 151.44 kcal/mol above the lowest dissociation channel. A sequential loss of two H atoms, first from the CH<sub>2</sub> site and then another H atom, have energies 122.73 kcal/mol (for the isomer 1), 122.14 kcal/mol (for isomer 2) and 123.23 kcal/mol (for isomer 9) above the lowest dissociation channel.

#### 2.5.4 Protonated Phenanthrene

Protonated phenanthrene provides an interesting and more complex counterpart to protonated anthracene in that it has five stable isomers, each of which can potentially contribute DIB features. Because of its complex potential energy surface, no tunneling and fewer dissociation pathways are calculated here (Figure 2.12, Table A.31 in Appendix A). Unlike the other protonated aromatic molecules discussed in this chapter, the protonated phenanthrene isomers are almost isoenergetic and are stable with respect to dissociation by 59.53 kcal/mol (1-C<sub>14</sub>H<sub>11</sub><sup>+</sup>), 57.53 kcal/mol (2-C<sub>14</sub>H<sub>11</sub><sup>+</sup>), 58.98 kcal/mol (3-C<sub>14</sub>H<sub>11</sub><sup>+</sup>), 58.46 kcal/mol (4-C<sub>14</sub>H<sub>11</sub><sup>+</sup>) and 59.33 kcal/mol (9-C<sub>14</sub>H<sub>11</sub><sup>+</sup>), respectively.

By analogy with protonated naphthalene and anthracene, the lowest dissociation channel for protonated phenanthrene is the loss of an H atom from the protonation site (0.00 kcal/mol). The loss of a proton from the CH<sub>2</sub> site lies 140.27 kcal/mol above the lowest dissociation channel and will not be considered further.

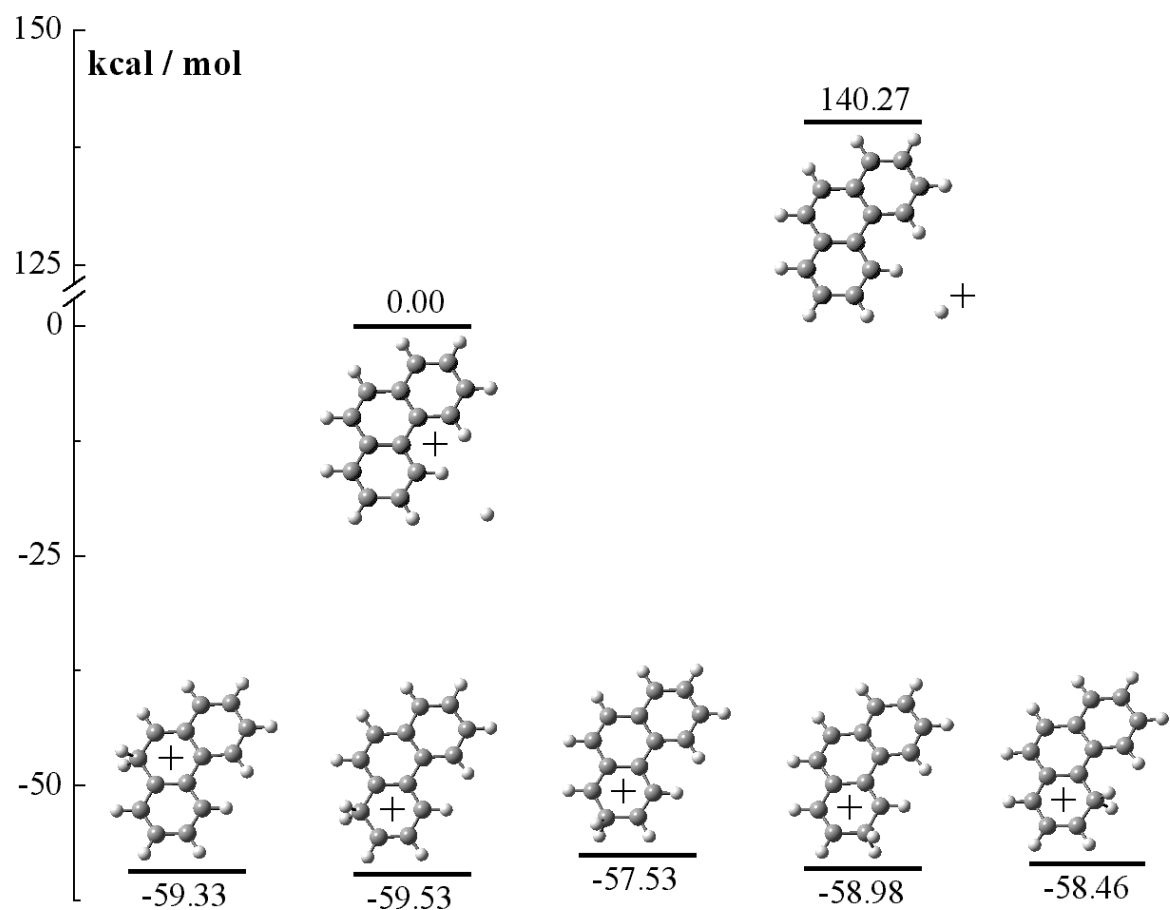


Figure 2.12: A simplified version of the protonated phenanthrene energy landscape.

### 2.5.5 Protonated Pyrene

Protonated pyrene has three isomers that are stable with respect to dissociation by 60.28 kcal/mol ( $1\text{-C}_{16}\text{H}_{11}^+$ ), 46.57 kcal/mol ( $2\text{-C}_{16}\text{H}_{11}^+$ ) and 50.52 kcal/mol ( $4\text{-C}_{16}\text{H}_{11}^+$ ) (Figure 2.13, Table A.32 in Appendix A). As with the smaller protonated PAHs, the lowest dissociation channel for protonated pyrene is calculated to occur via the loss of an H atom from the protonation site (0.00 kcal/mol). The loss of a proton from the  $\text{CH}_2$  site is 150.46 kcal/mol above the H atom loss channel.

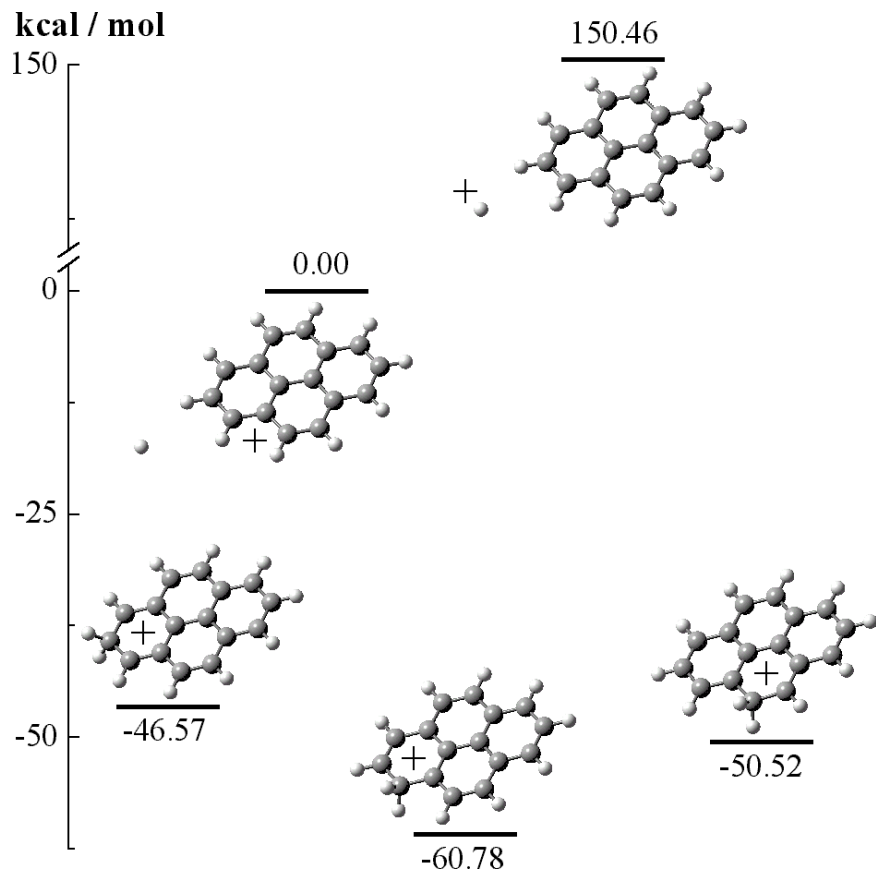


Figure 2.13: The energy landscape of protonated pyrene (not complete).

### 2.5.6 Hydrogenated PAHs

The main goal of this suite of calculations was to investigate the fate of protonated PAHs during electron recombination. Only the energies of hydrogenated PAH stable isomers and hydrogen loss channels were calculated, and only hydrogenated benzene, naphthalene, and anthracene were considered. The results are presented in Figures 2.14 – 2.16 and Tables A.33 – A.35 (Appendix A).

The lowest energy dissociation channel is the loss of a hydrogen atom from the CH<sub>2</sub> site, and as in the case for protonated PAHs, its energy was set to 0.00 kcal/mol. The next channel is the loss of an H<sub>2</sub> molecule from the hydrogenation site, and lies only 5.5 – 6.0

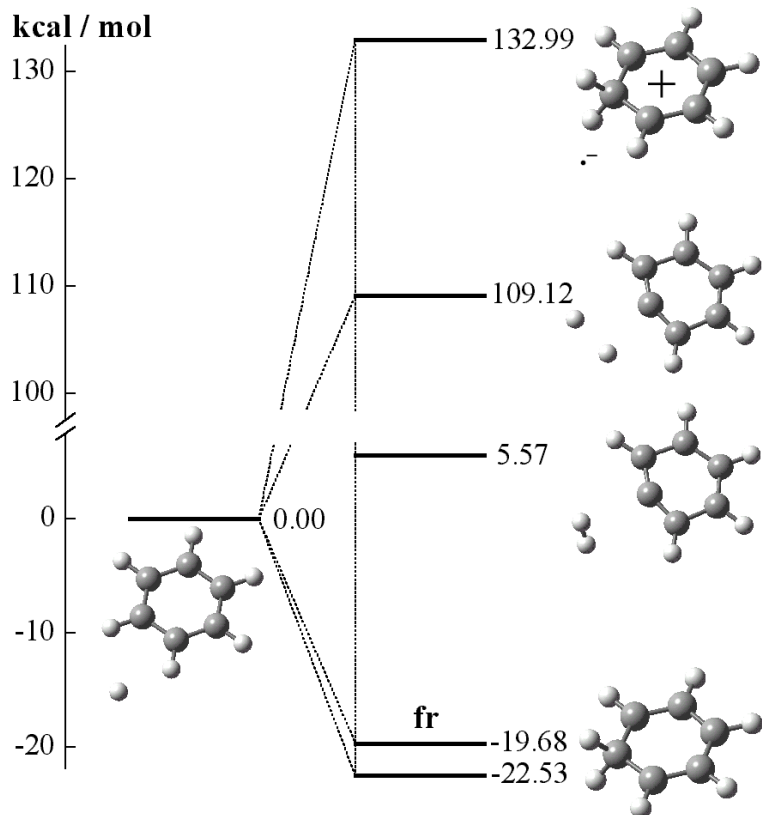


Figure 2.14: Hydrogenated benzene energy landscape.

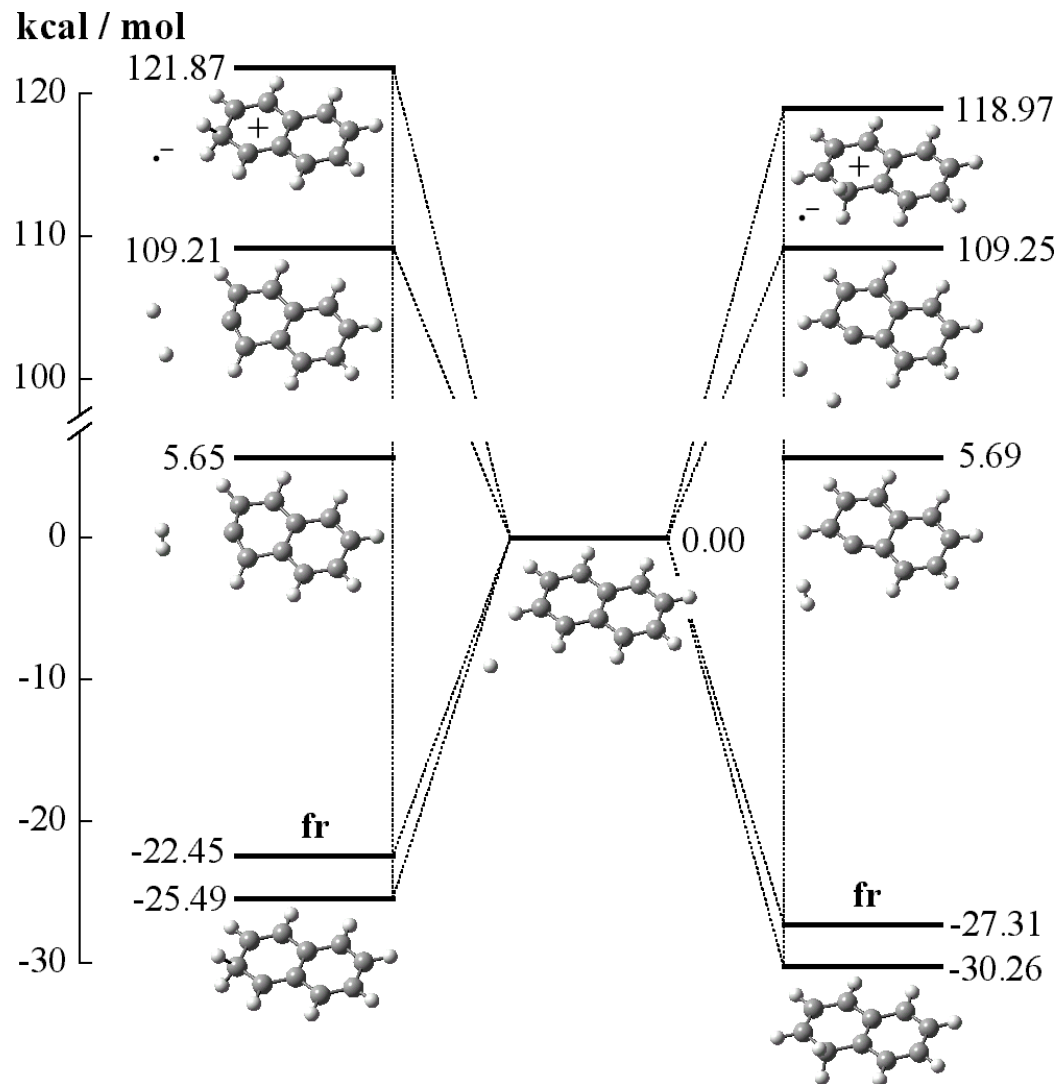


Figure 2.15: Hydrogenated naphthalene energy landscape.

kcal/mol higher in energy. A sequential loss of two hydrogen atoms, one of which is from the hydrogenation site – is almost 110 kcal/mol above the lowest energy channel.

Species labeled as **fr** (frozen) designate hydrogenated PAHs with geometries fixed to that of the protonated PAHs and energies that were corrected by ZPEs of protonated PAHs. Such geometries are not those appropriate for equilibrium, but rather, represent initial structures that are formed immediately after recombination. The energies of these structures are  $\sim 3$  kcal/mol above those of the equilibrium structures.

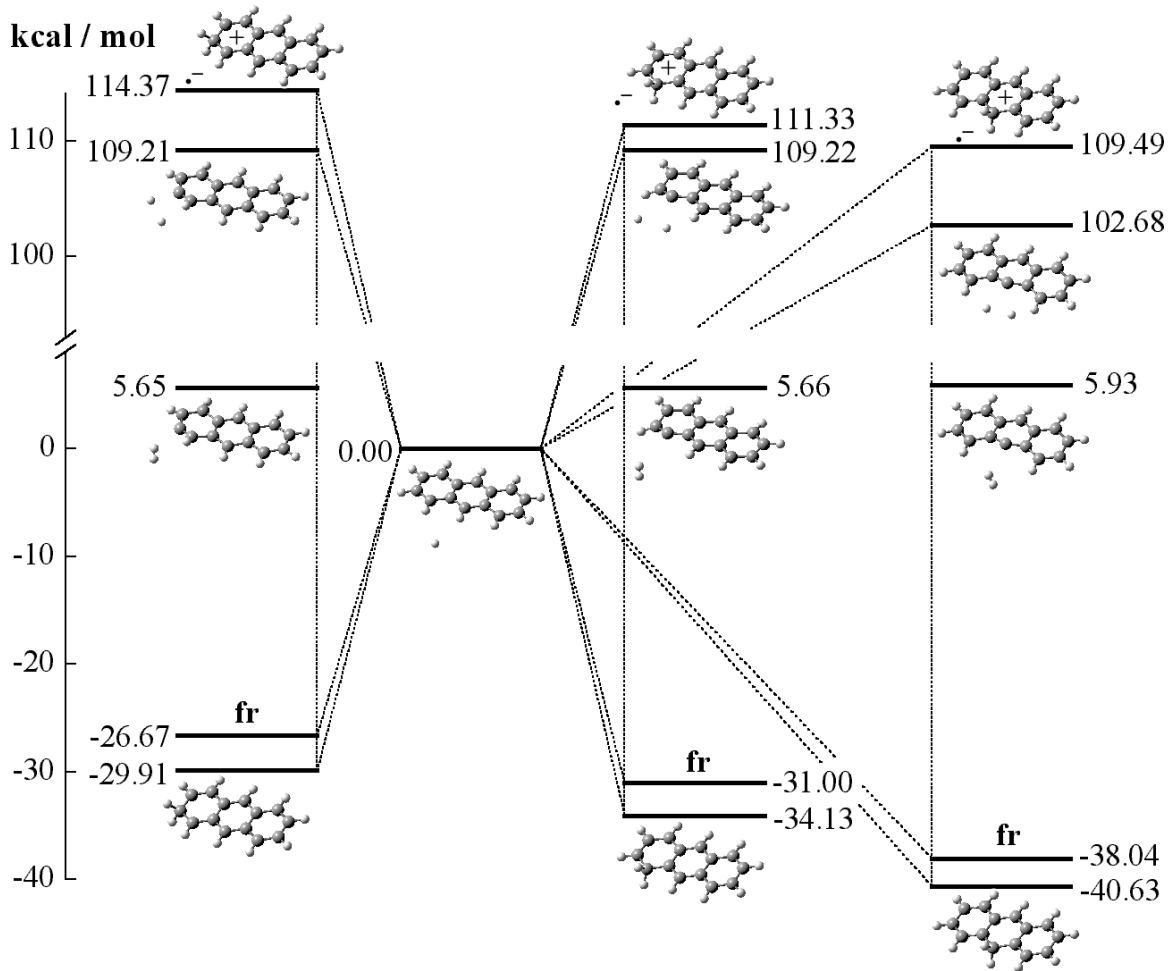


Figure 2.16: Hydrogenated anthracene energy landscape.

As a general trend, hydrogenated species become more stable with respect to dissociation as the size of the molecule grows. While hydrogenated benzene is stable by only 22.53 kcal/mol, isomers 1, 2 and 9 of hydrogenated anthracene are stable by 34.13, 29.91 and 40.63 kcal/mol, respectively. Since protonated PAHs have similar ionization energies, the amount of excess energy decreases with PAH size. For larger PAHs, the dissociation yield should drop substantially because the extra energy can be vibrationally distributed over the full molecule via IVR processes. In all cases, hydrogenated PAHs are less stable than protonated PAHs since they are not closed shell species.

## 2.6 Discussion

In regions of the interstellar medium exposed to ultraviolet photons (translucent clouds, H II regions, the diffuse medium), PAHs will exist in a variety of charge states. Anions typically have rapid photodetachment rates, and so cationic species are the most likely ionized form of interstellar PAHs. Neutral PAH precursors, for example, can acquire a positive charge either via ionization (UV or cosmic rays) or through the reactions with charged particles. In dense regions of the ISM such as molecular clouds, neutral PAH molecules can be protonated in collisions with  $\text{H}_3^+$  or  $\text{HCO}^+$ , thanks to their high proton affinities. Being closed-shell species, protonated PAHs are not as reactive as PAH cations – often referred as cation radicals – and would therefore be expected to be rather stable in the interstellar medium. This is reflected in the energetics of the cationic PAH species, with the above calculations demonstrating that protonated PAHs are more stable than their radical cation cousins. In addition, the observed laboratory reaction rates between H atoms and protonated benzene, naphthalene, pyrene, their cations, and dehydrogenated cations [75] all suggest that protonated PAHs can be created efficiently from radical cation precursors. Hence, if PAHs exist in the interstellar medium and can survive UV radiation, an extremely important component of the charge balance is likely to be carried by PAHs in their protonated form.

During protonation of aromatic molecules, the molecular symmetry decreases. This has important spectroscopic implications for the protonated PAHs as DIB and UIR carriers. For example, the IR spectrum of protonated PAHs should be more dense since more vibrational modes would be IR active. While there are no microwave spectra of neutral aromatic hydrocarbons and their cations (unless they heterocyclic forms are examined) due to their

lack of a permanent dipole moment (Appendix A, Table A.1), their protonated analogs do have significant dipole moments (at the protonation site) and should in principle be observable in the microwave with sufficient sensitivity. For example, 1–0 transition in protonated benzene should lie near  $\sim 8209$  MHz and could thus be searched for with standard FTMW techniques in the laboratory, as was successfully carried out for the phenyl radical  $C_6H_5$  [118].

### 2.6.1 Changes in the Vibrational Spectrum

IR vibrational spectra of PAHs change significantly upon protonation (Appendix A, Figures A.1 – A.19), most likely due to the reduction in the molecular symmetry [23] (Appendix A, Table A.1) and the concomitant increase in the number of allowed IR vibrational transitions. The biggest change is in the  $1100 - 1600\text{ cm}^{-1}$  range, where the neutral PAHs have only few, typically weak vibrations. The protonated PAHs, on the other hand, have their strongest lines in this region and the density of bands is high. Furthermore, the protonated PAH vibrational bands are located very close to  $6.2 - 6.3\text{ }\mu\text{m}$  and  $8.6\text{ }\mu\text{m}$  features in the interstellar UIR spectrum [23].

Another change is the dramatic decrease in the intensities of C–H stretch vibrations in  $3000 - 3100\text{ cm}^{-1}$  range and the appearance of new  $CH_2$  stretching vibrations that are not present at all in the neutral and cation spectra. The  $CH_2$  vibrations (symmetric and asymmetric stretches) are separated by  $1 - 20\text{ cm}^{-1}$  and located from  $2830 - 2910\text{ cm}^{-1}$ . Experimentally, it is these vibrations that were recorded in the cluster dissociation spectrum of protonated benzene–Ar [3, 96]. The  $CH_2$  vibrations are red-shifted from the aromatic C–H stretching modes and are located at wavelengths that can contribute to the red wing of  $3.29\text{ }\mu\text{m}$  ( $3040\text{ cm}^{-1}$ ) UIR feature. Since the exact frequencies depend on the

PAH molecule and the isomer, the CH<sub>2</sub> vibrational doublet from protonated PAHs will be difficult to observe astronomically, but these vibrations may well explain a part of, but not all, of the 3.29  $\mu\text{m}$  red wing [23, 96].

### 2.6.2 Proton Mobility

When a protonated PAH molecule is excited vibrationally but without sufficient energy to dissociate, it can isomerize by intramolecular proton transfer from one carbon atom to another. This behavior is uniquely inherent to protonated PAHs. Neutral PAHs and their radical cations do not possess this dynamical possibility, which may have important ramifications under interstellar conditions. Depending on the level of excitation, the proton migration may occur only between two adjacent isomers, within one carbon ring, or over the entire carbon framework. The proton can even migrate from one ring to another via a ring fusion carbon, though this can only occur at rather higher levels of internal excitation since the isomer protonated at the ring fusion is rather unstable. Proton tunneling across the ring fusion is possible only in protonated catacondensed PAHs (naphthalene, anthracene, phenanthrene, tetracene, etc.) In protonated pericondensed PAHs (pyrene, coronene, ovablene, etc.), the migration can only occur on the outside of the molecule via 2-ring fusion carbon isomers since the protonation at the inner, 3-ring fusion sites is energetically prohibitive.

The ratio of the protonated PAH isomers in the ISM during formation is most likely to be statistical. For naphthalene it would be 1 : 1 (isomer 1 : isomer 2); for anthracene – 2 : 2 : 1 (isomer 1 : isomer 2 : isomer 9); for phenanthrene – 2 : 2 : 2 : 2 : 1 (isomer 1 : isomer 2 : isomer 3 : isomer 4 : isomer 9); and for pyrene – 2 : 1 : 2 (isomer 1 : isomer 2 : isomer 4). If the protonated PAH ion is later excited vibrationally (collisionally or by radiation), it may

isomerize. In a large ensemble, this will scramble the initial isomer distribution and is most likely to change it closer to a thermodynamic equilibrium of isomers. On the other hand, the true thermodynamic equilibrium may be not attainable if the UV excitation rate is too high. The actual rate for reaching the equilibrium may be calculated only as a part of a model where isomerization rate dependence on the excitation energy is calculated for each isomer and then compared to the IR fluorescence lifetime. In general, the isomerization probability is the highest shortly after initial excitation, and then is reduced with every emitted IR photon.

Even in cold environments, the isomer distribution will not settle to the most stable isomer only. For example, in the case of interstellar methyl isocyanide, the amount of the metastable isomer  $\text{CH}_3\text{NCH}^+$  is predicted to be  $\sim 10 - 25\%$  of the amount for the stable isomer  $\text{CH}_3\text{CNH}^+$ , in spite of the isomer energy difference of 10 kcal/mol and the barrier of 65 kcal/mol [119].

Proton mobility also dramatically increases the density of the vibrational states once the internal energy rises above the isomerization barriers. Since these barriers correspond to  $\sim$ visible wavelength photons, the proton mobility in protonated PAHs may well lead to significant broadening of their electronic spectra, a topic discussed at greater length in Chapter 6. The photostability should also be greatly enhanced, which would lead to improved survivability of protonated PAHs under interstellar conditions.

### 2.6.3 Dissociation Channels

For protonated benzene, the lowest energy dissociation channel is the loss of the hydrogen molecule  $\text{H}_2$  from the protonation site, with an H atom loss not much higher in energy. The loss of 2 a.m.u. (either  $\text{H}_2$  or 2H) was observed in protonated benzene UV photodissociation

experiments [90].

According to the B3LYP calculations for polycyclic molecules, the lowest energy dissociation channel is the loss of a single hydrogen atom (H) from the protonation site, with the loss of a hydrogen molecule ( $H_2$ ) higher in energy by only 10 – 20 kcal/mol. Interestingly, only the loss of  $H_2$  molecules (or two H atoms) has been observed in the UV multiphoton dissociation of protonated anthracene and pyrene (Chapter 5). The sequential loss of two hydrogens was also observed in the CW visible photodissociation of coronene cations [120]. Both of these experiments illustrate the higher stability of the closed-shell protonated species compared to the open-shell cations. This stability also seems to be strongly influenced by the composition of the photodissociation products.

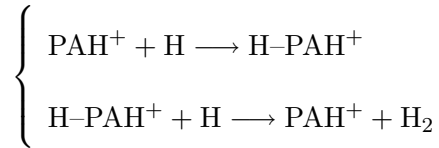
Other dissociation channels (H loss from non-protonation site, C–C bond cleavage or  $H^+$  loss) are much higher in energy and are therefore very unlikely to be important processes in interstellar photodissociation.

Typical dissociation energies for the two lowest channels are on the order of 50 – 80 kcal/mol (2.2 – 3.5 eV or  $\lambda \sim 600$  – 360 nm for a single photon). Thus, from energetic considerations alone, protonated PAHs should be able to dissociate even from the absorption of visible or near-UV photons. In Chapter 3, the energies for the excited states will be calculated, with Chapters 5 and 6 turning to experimental analyses of the photostability and spectra of protonated PAHs.

#### 2.6.4 Interstellar $H_2$ Formation

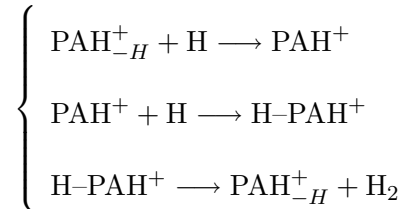
Molecular hydrogen is abundant in the interstellar medium. The mechanisms of  $H_2$  formation are still debated in the literature, especially in warm regions such as diffuse or translucent clouds where dust grain synthesis models have a very difficult time generating

sufficient rates of molecular hydrogen production. One possible ‘out’ is through reactions of PAHs with atomic hydrogen since the effective ‘surface area’ is increased dramatically. From the bond dissociation energies and barrier heights calculated for benzene and naphthalene [117], it is thought that hydrogen atom association reactions with PAH cations and dehydrogenated cations do not have a barrier. From these calculations, it was also suggested that H<sub>2</sub> abstraction by H atoms from protonated PAHs might occur efficiently. This mechanism was later extended to anthracene and pyrene molecules [121], and the general cycle would be:



The first step in this mechanism proceeds almost at collision rate, but the rate for the second step is not known. It should only be a fraction of the collision rate, even if it is almost barrierless since the reaction will proceed only if the hydrogen atom approaches the ‘right’ carbon at a proper angle.

Another way to form molecular H<sub>2</sub> is via protonated PAH dissociation to generate the dehydrogenated PAH cation, as has been suggested in discussions of PAH cation reactivity with H atoms (for benzene and naphthalene [76]). The cycle for this mechanism would be:

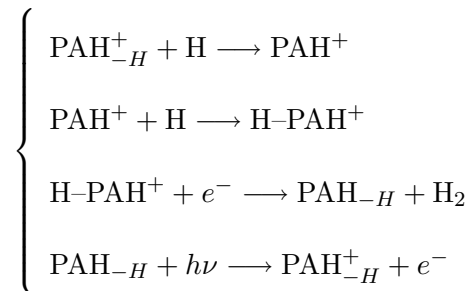


The first two steps in this reaction are exothermic and fast (they occur at nearly the collision rate), but the last step is endothermic. Thus, it is the rate-determining step in this cycle and depends largely on the external sources of protonated PAH excitation in the ISM. The absorption of UV photons may provide a viable option in diffuse clouds or near luminous

young stars [90]. Chapter 5 discusses this in greater detail.

Whichever of the two mechanisms that predominates will depend on the rate for the second step in the first mechanism and the UV flux in the second cycle. Most likely, the first mechanism would be preferred since protonated PAHs were found to be photostable (Chapter 5).

One additional way to make molecular hydrogen would be through the H<sub>2</sub> loss channel by hydrogenated PAHs, formed in protonated PAH electron recombination. This channel is only 5.5 – 6.0 kcal/mol above the H atom loss channel. It should be energetically accessible since such dissociative recombination reaction for protonated PAHs should be exothermic by ∼100 kcal/mol. Dehydrogenated PAHs formed in this reaction would be ionized and would acquire hydrogen atoms to reform the protonated PAHs:



Such a cycle would be especially effective for smaller PAHs and would be facilitated by relatively high electron densities such as those found in diffuse clouds where the fractional electron abundance of  $f(e^-) = n(e^-)/n(H) \sim 10^{-4}$  is maintained by atomic carbon photoionization.

## 2.7 Summary

The above calculations show that protonated PAHs are stable species. They are formed by proton binding to a carbon atom and not the C–C bond or the whole aromatic ring. In the ISM, PAHs are likely to be in protonated form.

Protonated PAHs have a stronger and more complicated IR spectrum than neutral PAHs. Some of the strong IR frequencies are located near UIR bands in the mid-IR range. CH<sub>2</sub> stretch vibrations are located in the red wing region of 3.3  $\mu\text{m}$  UIR feature and may account for part of it.

The two lowest dissociation channels are loss of an H atom and an H<sub>2</sub> molecule from the protonation site. The dissociation energies are in the range 50 – 80 kcal/mol and in principle may be accessed by near UV or visible photons. The H<sub>2</sub> loss channel may be responsible for molecular hydrogen production in the ISM.

Vibrationally excited protonated PAHs can isomerize without dissociation. The proton can migrate almost everywhere on the outside rim of the PAH molecule. This would lead to broader electronic spectra and possibly to the thermodynamic distribution of the isomers in the ISM.